Volume 4, Issue 3, 2014, 731-735 **ISSN 2069-5837**

Biointerface Research in Applied Chemistry

www.BiointerfaceResearch.com

Review Article **Open Access Journal**

Received: 30.11.2013 / Revised: 01.03.2014 / Accepted: 31.03.2014 / Published on-line: 15.06.2014

Towards optimizing metal enhanced fluorescence (MEF) for improved detection of disease biomarkers

Anthony Centeno[1,*], Fang Xie[2]

[1]iKhoza Nano-Characterization, Structural Control and Processing, Malaysia-Japan International Institute of Technology, University Technology Malaysia International Campus, 54100 Kuala Lumpur, Malaysia

[2]Department of Materials, ImperialCollegeLondon, Exhibition Road, SW7 2AZ, UK

*corresponding author e-mail address:***acenteno@ic.utm.my**

ABSTRACT

Fluorescent molecules are commonly used for the detection of disease biomarkers. Metal Enhanced Fluorescence (MEF) is a promising strategy for improving the detection sensitivity. This paper describes current research on using Computational Electromagnetics (CEM) as a prediction tool for fluorescent enhancement. Recent published work has shown that for isolated spherical nanoparticles in solution fluorescent enhancement can be predicted with reasonably good accuracy. This work has been extended to consider immobilized particles in periodic arrays formed by colloidal lithography. These kinds of arrays could have potential applications in sensing and bioimaging. The initial results show that coupling between the fluorophore and the metal nanoparticle is extremely complex. The coupling is strongly dependent on the position and electromagnetic polarization of the fluorophore emission with respect to the adjacent metal surface.

Keywords: *Fluorescence, Metal Enhanced Fluorescence, Electromagnetic Modelling, Nanoparticles.*

1. INTRODUCTION

The use of fluorescent molecules is currently the most common labeling technique in biosensing for the detection of disease biomarkers [1]. Such approaches have seen widespread use in clinical practice, one example being Enzyme Linked Immunosorbent Assay (ELISA) [2]. It would be extremely beneficial to improve the detection sensitivity and the amplification of light from fluorophores and the coupling to metal nanostructures [3-5]. Metal Enhanced Fluorescence (MEF) is a promising strategy for achieving this. Metal nanostructures have long been researched due to their ability to manipulate incident light. In this article the process of MEF will be discussed using computational modeling and previously published results. Essentially all uses of fluorescence depend on the spontaneous emission of photons in all directions linked to radiative decay rates. An effective change in the radiative decay rate was observed when fluorophores were placed in close proximity to metal colloids [3].

Vukovic et al. [4] described the overall influence of a metal nanoparticle in three stages. The first stage is the absorption of exciting light by the molecule which is enhanced by the Localized Surface Plasmon Resonance (LSPR) of the metal nanoparticle. Once in an excited state the molecule undergoes internal processes to transit into the emitted excited state. Although the metal can modify these processes they are usually very fast compared to other processes and are not usually considered in the MEF mechanism. The final step is when the molecule decays to the ground state through the emission of a photon, either radiatively or nonradiatively. The metal will modify the radiative decay rate and create new channels of nonradiative decay, through energy and charge transfer between the molecule and metal. It would appear likely that the intrinsic nonradiative decay rate of the molecule is also modified, but the new nonradiative channels mask this effect [4].

The quantum yield of an isolated fluorophore molecule is given by [6]:

$$q^O = \frac{\gamma_r^O}{\gamma_r^O + \gamma_{nr}^O} \quad (1)$$

where γ_r^O and γ_{nr}^O are the radiative and non-radiative decay rates respectively. The superscript ^{O}means that the fluorophore is isolated, rather than in the presence of a metal nanoparticle.

In the presence of a metallic particle there is an additional radiative channel, and an absorption channel. The modified quantum yield is then given by [6]:

$$q^m = \frac{\gamma_r^m / \gamma_r^O}{\gamma_r^m / \gamma_r^O + \gamma_{abs}^m / \gamma_r^O + (1-q^O)/q^O} \quad (2)$$

Combining (1) and (2) gives:

$$q^m = \frac{\gamma_r^m}{\gamma_r^m + \gamma_{abs}^m + \gamma_{nr}^0} \quad (3)$$

and the lifetime, τ^m, is be given by:

$$\tau^m = \frac{1}{\gamma_r^m + \gamma_{abs}^m + \gamma_{nr}^O} \quad (4)$$

The excitation rate of the fluorophore occurs due to the large electromagnetic field enhancement, caused by the excitement of the LSPR of a metal nanoparticle by incident photons at the resonant wavelength. The excitation rate is found by considering the local electric field at the position, wavelength of excitation,

$E(x_d, \lambda_{ex})$ and the emitters orientation, e_p. If we consider the electric field in the presence of the metal nanoparticle near the fluorophore then the excitation rate enhancement is given by [6]:

$$X = \frac{\left|E(x_d, \lambda_{ex}) e_p\right|^2}{\left|E_i\right|^2} \qquad (5)$$

where Ei is the incident free space electric field without the nanoparticle present. The fluorescent rate enhancement is now given by:

$$\Psi_{enh} = X \frac{q^m}{q^O} \qquad (6)$$

For MEF almost all structures being explored consist of either silver (Ag) or gold (Au), since their LSPR is in the visible or near infrared part of the electromagnetic spectrum.

2. TOWARDS ACCURATE PREDICTION OF MEF USING ELECTROMAGNETIC ANALYSIS

2.1. Computational Procedure

The electromagnetic analysis described here is carried out using the Finite Difference Time Domain (FDTD) technique [7]. It should be noted that electromagnetic analysis can be carried out using other computational electromagnetic techniques, such as Finite Element [8] or Discrete Dipole Approximation [9]. FDTD has been chosen because it is relatively straightforward to implement and can be easily extended in the future to include substrate materials, nanoparticles of multiple materials and different shaped particles [6]. Further time domain modeling followed by a Fourier transform will automatically generate solutions over a wide spectral bandwidth in a single simulation

To obtain values of modified quantum yield and fluorescent rate enhancement we need to calculate the decay rates γ_r^m, γ_{abs}^m and γ_r^0. This is accomplished by considering the spontaneous emission of the fluorophore as a small electric dipole [10], [11], [12]. If we consider the electric fields generated by a small electric dipole then these decay rates can be found in terms of the Poynting vector as described previously [6] such that:

$$\gamma_r = \frac{\int_s \mathrm{Re}\left(\mathbf{E_T} \times \mathbf{H_T}^*\right) da}{2} \qquad (7)$$

and

$$\gamma_{abs}^m = \frac{-\int_s \mathrm{Re}\left(\mathbf{E_S} \times \mathbf{H_S}^*\right) da}{2} \qquad (8)$$

where s is a surface that encloses the fluorophore molecule (small dipole) and the particle. In equation (7) we consider the total electric and magnetic field crossing s, whereas in equation (8) it is the scattered fields that are considered, hence the subscripts T and S for **E** and **H**. To find γ_r^0 from equation (7) only the small dipole has to be considered in the calculation, whilst to find γ_r^m the metal nanoparticle is added to the model and enclosed by the surface.

The metal nanoparticles were modeled using the combined Drude-Lorentz model[13]:

$$\varepsilon(\omega) = \varepsilon_\infty + \sum_{i=1}^{n} \frac{\alpha_i \omega_p^2}{\omega_{oi}^2 - \omega^2 - j\omega\tau_i} \qquad (9)$$

Where ω_p is the plasma frequency, α the oscillators' strength, $\omega_o$the resonant frequency of each oscillator, j the imaginary unit and τ the damping frequency of each oscillator. In our calculations we have used one Drude and five Lorentz terms in the summation. The parameters used for Au and Ag were obtained from Rakic et-al [13]. The FDTD mesh discretization was optimized by convergence testing and it was found that a resolution between 1 and 1.5 nm is required for good accuracy. The time step, Δt, was given by $\Delta t = S\Delta x$, where S was the Courant factor. In all the FDTD calculations a Courant factor of 0.5 was used. This was found to provide stable and convergent simulations in all cases. The field source used was a Gaussian pulse.

2.2. Isolated Spherical Particles

This section summarizes previous work on isolated spherical nanoparticles first reported by Centeno, Xie and Alford in reference [7]. Fluorescent enhancement due to isolated Au and Ag nanosphere was calculated using the Finite Difference Time Domain technique. When calculating γ_r^m and γ_{abs}^m the small dipole is modeled by placing an electric field source close to the nanosphere and polarizing it either normal (**E_n**) or tangentially (**E_t**) to the sphere surface, as depicted in Figure 1.

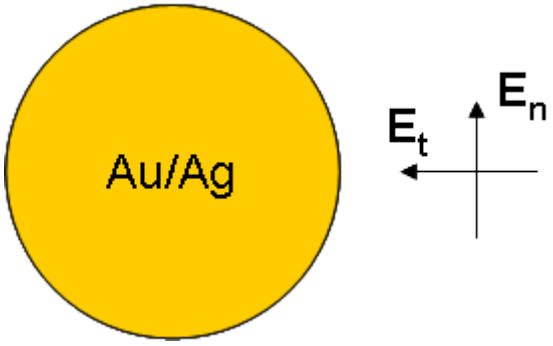

Figure 1. The fluorescent molecule is modelled by placing an electric field source polarized either normal or tangentially to the surface of the sphere.

The objective is to calculate $\Psi_{enh}$for commercially available fluorescent dyes, a number of which are considered here. In the

calculations, $\Psi_{enh}$are found for different separations between the metal sphere and the fluorophore molecule. For each case the excitation rate at the maximum absorption wavelength and the modified quantum yield for the maximum emission wavelength are used. Figure 2a shows the results of fluorescent rate enhancement obtained for Au and Figure 2b for Ag. In an attempt to provide a qualitative validation, a comparison was made with the experimental data presented in reference [10]. If Ag spheres and Alexa488 are considered the enhancement in the FDTD calculations are 3.9 at 5 nm , 2.9 at 10 nm and 2.1 at 20 nm, compared to 4, 2.7 and 2 respectively [10]. For Au spheres experimental data is available for Nile Blue and presented in reference [10]. The FDTD calculations show enhancement values of 7.2 at 5 nm, 5.5 at 10 nm and 3.6 at 20 nm, compared to the published experimental values of 3.5, 2.8 and 1.8 respectively. It should be noted that the experimental data has been approximately extrapolated from reference [10] and there is an expected margin of error in the comparison of around 0.2.

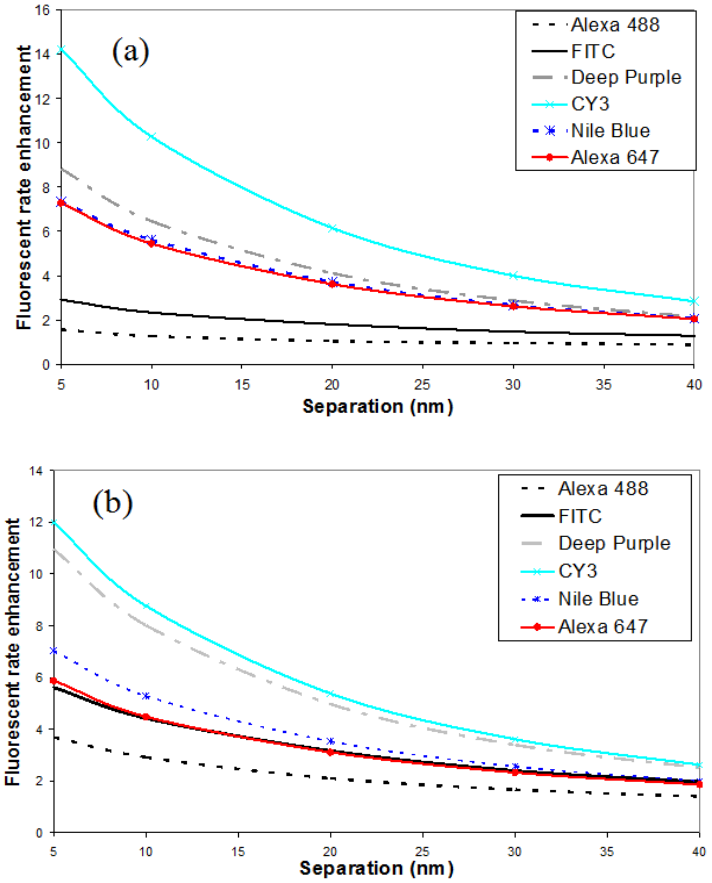

Figure 2. Fluorescent enhancement rate (Ψ_{enh}) calculated using FDTD for various commercial fluorescent dyes, assuming excitation at the maximum excitation wavelength, emission at the maximum emission wavelength and maximum quantum yield. The spheres are 80 nm diameter (a) Au and (b) Ag.

Considering these results it can be seen that for the Ag/Alexa488 case there is a reasonably good comparison whilst the FDTD calculations predict almost exactly double the enhancement rate for the Au/Nile Blue case. This difference was attributed to the experimental results using an excitation wavelength above the excitation maximum which has been used in the calculations, hence a subsequent uncertainty in q^0. This is the main problem in accurate predictions of the fluorescent enhancement rate, since the excitation wavelength used in measurements is unlikely to be exactly at the excitation maximum of the dye but rather at a suitable laser frequency. Nevertheless the comparisons are considered good enough to make qualitative judgments on which dyes will produce the best fluorescent enhancement.

2.3. Immobilized Particles

Immobilizing the metal nanoparticles and being able to define their shape, size and separation is an active area of research. By controlling these factors the MEF can be made repeatable, which is important for diagnostics [1]. Recent results using both Au and Ag nanoparticles in close packed hexagonal arrays, as depicted in Figure 3, have shown promising MEF of up to 2 orders of magnitude [14],[15]. The arrays discussed here can be fabricated using colloidal lithography. Colloidal lithography has the advantages of being quicker and more cost effective than electron beam lithography. It exploits the deposition of colloidal particles, typically polystyrene spheres, as masks for lithography. Colloidal lithography is a large area, robust, parallel and cheap method.

As depicted in Figure 3 the nanoparticles are triangular-like but have concave sides. There is strong electromagnetic coupling between the nanoparticles. In Figure 4 the calculated electric field enhancement at 780 nm is shown for Au nanoparticles formed using 300 nm diameter polystyrene spheres as the masks for the lithography. Xie et al [14] tuned the particle size and interparticle distance using oxygen plasma etching of the polystyrene template and obtained a fluorescent enhancement of 68 for Alexa Fluor® 790 using gold nanoparticles of tip-to-tip dimensions of 80 ± 5.9 nm, inter-particle separation of 62.5 ± 13.5 nm and height 100 nm (approximately the same dimensions as the FDTD model used in Figure 4). Since the fluorescent enhancement is due to both excitation enhancement of the fluorophore, caused by large localized electric fields, and emission enhancement it is important to consider both.

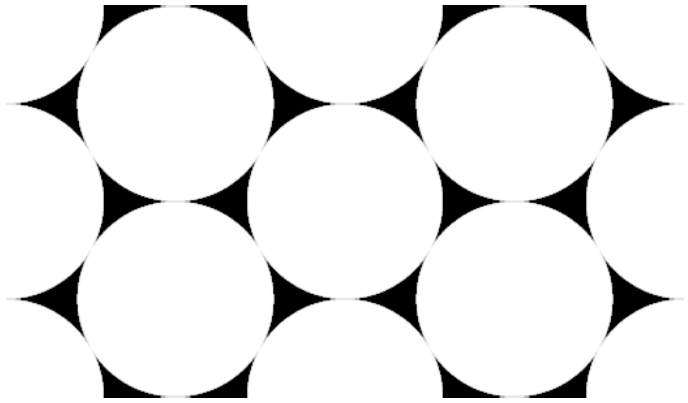

Figure 3. Triangular like nanoparticle arrays that can be formed using polystyrene spheres as a template in colloidal lithography.

For the isolated spherical particle discussed in section 2.2 it is comparatively straightforward to estimate the emission

enhancement, since there is spherical symmetry. For the shapes formed using colloidal lithography there is much less symmetry to exploit. Nevertheless it is possible to gain some insight by considering different positions around the triangular structure. Here an FDTD model is used, where the fluorophore was placed in three positions around the nanoparticle and a height of 10 nm from the glass surface. The three positions are shown in Figure 5. P1 and P3 are positioned 10 nm from the adjacent tips of the triangular-like structure. P2 is 10 nm from the mid-point of the concave side.

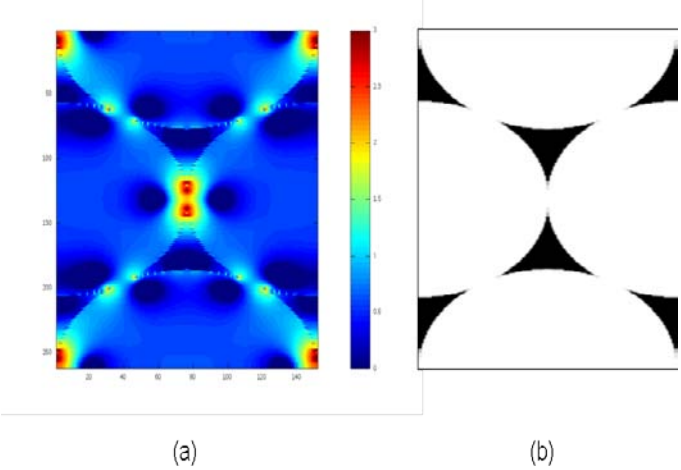

Figure 4. (a) The electric field enhancement at 780 nm due to an array of Au nanoparticles. The tip-to-tip dimensions of the nanoparticles are 82 nm and the height is 100 nm. The field is calculated mid-way up the nanoparticle. (b) A depiction of the position of the metal nanoparticles. From (a) and (b) it can be seen that the e-field enhancement is up to 3 orders of magnitude in the separation between the nanoparticles (Note the scale is logarithmic).

The emission enhancement (q^m/q^0) for commercially available dyes was calculated for the three positions, as summarized in Table 1. It can be seen that the modified quantum yield is strongly dependent upon position and polarization. It can also be seen that the emission enhancement from a fluorophore is very position and polarization dependent for this shape of nanoparticle. It is evident that if AF790 is considered, most of this enhancement is attributed to the increased intensity of the local electric field based upon the results from reference [14] of a fluorescent enhancement of 68.

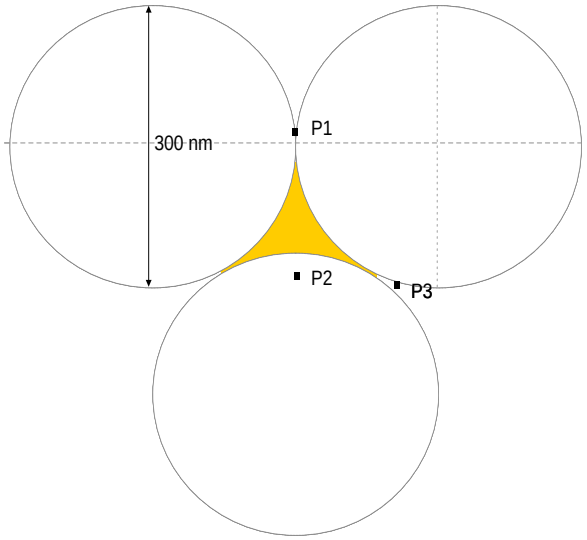

Figure 5. Illustration of the concave sides of the triangular like nanoparticles formed by polystyrene nanospheres and an indication of the three positions used to calculate the emission enhancement of fluorophore molecules. The calculation of which is given in Table 1.

Table 1. Emission enhancement at the three positions of nanoparticle depicted in Figure 5 for five different commercial fluorescent dyes.

Alexor Fluor® Dye	Quantum Yield of Dye (q^0)	Emission Enhancement (q^m/q^0) for different positions and polarization of fluorophore.				
		P1, normal polarization	P1, tangential polarization	P2, normal polarization	P3, normal polarization	P3, tangential polarization
AF 488	0.92	0.6	0.34	0.85	0.97	0.985
AF 555	0.1	3.86	0.76	2.77	0.75	0.879
AF 647	0.33	1.43	0.54	1.65	0.518	0.77
AF 700	0.25	2.24	0.6	2.03	0.48	0.69
AF 790	0.1	7.5	1	3.7	0.675	1.35

3. DISCUSSION

In practice it would be very advantageous to be able to use arrays of immobilized particles on a substrate. These could be easily manufactured and have known performance that is repeatable. It would be desirable to manufacture the arrays such that the fluorescent enhancement was maximized but this requires an understanding of the emission enhancement mechanism.

In this paper a short review is presented on MEF and the use of electromagnetic modeling tools to predict the level of fluorescent enhancement. For simple isolated shapes with high levels of symmetry it has been shown that it is possible obtain reasonably accurate levels of prediction. When more complex shapes are considered in immobilized arrays, it is seen that the emission enhancement from fluorophore molecules is strongly dependent upon the position and polarization of the emission. The results suggest that electric field enhancement is the main mechanism for fluorescent enhancement and so the excitation wavelength of the dyes should be close to the localized surface plasmon resonance of the nanoparticles. However, this may be an over simplified view, since there may also be increased absorption at this wavelength. More work is required to fully understand the coupling mechanisms between the fluorophore and metal surfaces of nanoparticles. Future work will focus on using simpler shapes with rotational symmetry, cylinders for example, to understand this mechanism fully and then extend to more complicated shapes,

such as the concave sided triangles considered here. The eventual aim is to design optimized MEF arrays for disease biomarker detection.

4. CONCLUSIONS

Computational electromagnetic modeling can be used to predict fluorescent enhancement from individual fluorophores in close proximity to metal nanoparticles. By fully understanding the coupling process it is expected that optimized MEF arrays can be designed and developed in the future for the improved detection of various disease biomarkers.

5. REFERENCES

[1]Darvill D., Centeno A., Xie F., Plasmonic Fluorescence enhancement by metal nanostructures: shaping the future of bionanotechnology, *PCCP*, **2013**.

[2]Ambrosi A., Airo F., Merkoci A., Enhanced gold nanoparticle based ELISA for a breast cancer biomarker, *Analytical Chemistry*, 82, 1151-1156, **2012**.

[3]Lakowicz J R., Radiative decay engineering: biophysical and biomedical applications, *Anal. Biochem*., 298, 1-24, **2001**.

[4]Vukovic S., Corni S., Mennucci B,, Fluorescence enhancement of chromophores close to metal nanoparticles, *The Journal of Physical Chemistry C*, 113, 121-133, **2008**.

[5]Xie F., Baker M S., Goldys E M., Homogeneous silver-coated nanoparticle substrates for enhanced fluorescence detection, *J. Phys. Chem*., 110, 23085-23091, **2006**.

[6]Centeno A., Xie F., Alford N., Predicting the fluorescent enhancement rate by Au and Ag nanospheres using FDTD analysis, *IET Nanobiotechnol*., 7, 2, 50–58, **2013**.

[7]Oskooi A F., Roundy D., Ibanescu M., Bermel P., Joannopoulos J D., Johnson S G., MEEP: A flexible free-software package for electromagetic simulations by the FDTD method, *Comput. Phys. Commun*., 181, 687-702, **2010**.

[8]Khoury C G., Norton S J., Vo-Dinh T., Plasmonics of 3-D nanoshell dimmers using multipole expansion and finite element method, *ACS Nano*, 3 (9), 2776-2788, **2009**.

[9]Draine B T., Flatau P J., Discrete-dipole approximation for scattering calculations. *J. Opt. Soc. Am*. 11, 1491, **1994**.

[10]Bharadwaj P., Novotny L.,Spectral dependence of single molecule fluorescence enhancement, *Optics Express*, 15, 14266-14274, **2006**.

[11]Liaw J W., Chen C S., Chen J H., Plasmonic effect of gold nanospheroid on spontaneous emission, *PIER B*, 31, 283-296, **2011**.

[12]Chowdhury M H., Pond J., Gray S K., Lakowicz J R., Systematic computational study of the effect of silver nanoparticle dimmers on the coupled emissions from nearby fluorophores, *J. Phys. Chem. C*, 112, 11236-11249, **2008**.

[13]Rakic A D., Djurisic A B., Elavar J M., and Majewski M L., Optical properties of metallic films for vertical-cavity optoelectronic devices, *Appl. Opt*.. 37, 5271-5283, **1998**.

[14]Xie F., Centeno A., Ryan M P., Riley D J., Alford N M., Au nanostructures by colloidal lithography: from quenching to extensive fluorescence enhancement, J. Mater. Chem. B, 1, 536, **2013**.

[15]Xie F., Pang J S., Ryan M P., Riley D J., Alford N M., Nanoscale control of Ag nanostructures for plasmonic fluorescence enhancement of near-infrared dyes, Nano Research, 6(7), 496–510, **2013**.

6. ACKNOWLEDGEMENTS

This work has been possible due to the financial support of an EPSRC (UK) overseas collaboration fund. Dr Centeno also wishes to acknowledge the support provided by Imperial College through the award of an Honorary Research Fellow visiting position in the Materials Department.